A nonequilibrium golden rule formula for electronic state populations in nonadiabatically coupled systems

Rob D. Coalson,[a] Deborah G. Evans,[a] and Abraham Nitzan[b]
Institute for Advanced Study, Hebrew University, Jerusalem 91904, Israel

(Received 15 February 1994; accepted 21 March 1994)

A formula for computing approximate leakage of population from an initially prepared electronic state with a nonequilibrium nuclear distribution to a second nonadiabatically coupled electronic state is derived and applied. The formula is a nonequilibrium generalization of the familiar golden rule, which applies when the initial nuclear state is a rovibrational eigenstate of the potential energy surface associated with the initially populated electronic state. Here, more general initial nuclear states are considered. The resultant prescription, termed the nonequilibrium golden rule formula, can be evaluated via semiclassical procedures and hence applied to multidimensional, e.g., condensed phase systems. To illustrate its accuracy, application is made to a spin–boson model of "inner sphere" electron transfer. This model, introduced by Garg *et al.* [J. Chem. Phys. **83**, 4491 (1985)] for the nonadiabatic transition out of a thermal distribution of states in the initial (donor) electronic level, is extended to include nonequilibrium, nonstationary initial nuclear states on the donor surface. The predictions of the nonequilibrium golden rule are found to agree well with numerically exact path integral results for a wide range of initial distortions of the initial nuclear wave packet from its equilibrium configuration.

I. INTRODUCTION

The motion of molecules on electronically excited potential surfaces plays a major role in fundamental processes such as photochemistry and electron transfer. A very common, and often essential, feature of excited state dynamics is the coupling of motion on two or more Born–Oppenheimer potential surfaces. This interaction may result from spin–orbit coupling,[1] breakdown of the Born–Oppenheimer approximation,[2] coupling between molecular centers that gives rise to electron transfer, etc. The consequence is the transfer of occupation probability from one electronic state to another. Such phenomena play a major role in linear and nonlinear spectroscopies,[3] relaxation rates and quantum yields,[4] electron transfer,[5(a),(b)] and other nonadiabatic chemical rate processes.[5(c)]

While curve-crossing phenomena play an important role in excited state dynamics of isolated small molecules (e.g., photodissociation of ICN,[6] methyl iodide,[7(a)] and alkali halides[7(b)]), most chemically interesting processes take place in condensed phases. Coupling to the condensed phase solvent greatly complicates the relevant solute quantum dynamics. Exact solution of the Schrödinger equation is in general impossible. Reliable and efficient approximation procedures are needed.

Of central importance in the theory of condensed phase rate processes is the golden rule (GR).[8] Application of this procedure to the computation of electronic population dynamics in systems characterized by nonadiabatic transitions between different electronic states requires certain conditions. First, the interstate coupling should be small, since at the heart of the golden rule is an application of low order time-dependent perturbation theory. Many experimentally relevant systems fall in this category, which in the context of electron transfer is known as the nonadiabatic regime. Second, the golden rule assumes that the system is prepared in a rovibrational eigenstate of the initially populated electronic potential surface, or that the population on that surface is maintained in thermal equilibrium throughout the nonadiabatic relaxation process. The latter condition holds, irrespective of the initially prepared state, provided that thermal equilibration takes place on the initial surface on a time scale much shorter than the characteristic time required for significant changes in the electronic population. Under these conditions, the standard golden rule provides a simple formula for the rate constant,[9] which can be expressed as a time integral over a function (to be termed a time kernel) determined by sequential propagation of nuclear coordinate wave packets or density matrices on the two coupled surfaces. While exact evaluation of the relevant time kernels is in general not possible, a variety of semiclassical techniques have been developed,[10–12] and recent implementations[11,12] suggest that they can be applied successfully to many condensed phase problems.

The standard golden rule (GR) is also useful for a particular limit of nonequilibrium nuclear dynamics. In this limit, thermal relaxation is not necessarily fast relative to the nonadiabatic transition, but thermal dephasing is. In this case, only diagonal elements of the nuclear density matrix are relevant[13] and the time evolution is described by a master equation in the space of the nuclear level populations in the initial electronic state, where each such level decays because of the nonadiabatic coupling to the other electronic states with the rate determined by the standard GR formula. We note that vibrational dephasing is indeed much faster than vibrational relaxation for small molecules in the condensed phase at room temperature.[14] The same observation has also

[a]Permanent address: Department of Chemistry, University of Pittsburgh, Pittsburgh, Pennsylvania 15260.
[b]Permanent address: School of Chemistry, Sackler Faculty of Science, Tel Aviv University, Tel Aviv, 69978, Israel

 0021-9606/94/101(1)/436/13/$6.00 © 1994 American Institute of Physics

Downloaded 17 Mar 2004 to 132.66.16.34. Redistribution subject to AIP license or copyright, see http://jcp.aip.org/jcp/copyright.jsp

been made for several cases involving large solute molecules.[15]

In the most general nonequilibrium situation, the initial distribution in nuclear space is characterized not only by nonequilibrium populations, but also by coherences. For example, a sudden electronic transition from the lowest vibrational level of the ground electronic state produces a Gaussian wave packet on the excited potential surface. The subsequent adiabatic evolution of such a wave packet involves determininstic motion, thermal relaxation, and thermal dephasing of the nuclear motion. The effect of these nonequilibrium processes in the initially occupied excited electronic state on its subsequent time evolution can be most generally taken into account within generalized master equation models, where time evolution of coherences and possible non-Markovian effects are taken into account.[16] While being a very powerful *phenomenological* approach, this method cannot be used in computations involving realistic model systems, particularly in condensed phases. On the other hand, the adiabatic evolution of the initially prepared nuclear wave packet can be calculated using time dependent quantum or semiclassical methods. In this paper, we consider nonadiabatic electronic transitions in the presence of such nonequilibrium time evolution on the initial electronic surface. Provided that the backflow from the initially unoccupied electronic state to the initially occupied one can be neglected (a condition for the validity of the standard GR at long times), we find that it is possible to modify the standard GR prescription in a simple way in order to treat electronic population relaxation in the case of nonequilibrium preparation of the initial electronic state. The result, to be denoted as the nonequilibrium golden rule (NGR) formula, is only marginally more elaborate than the standard equilibrium version and is amenable to calculation by the same semiclassical techniques that have been successful in the equilibrium case. A similar approach in a more limited framework was suggested previously by Nitzan and Jortner;[17] however, no tests of its validity were carried out.

As a result of second order time dependent perturbation theory, the golden rule can only guarantee accuracy in its prediction of short-time dynamics. More sophisticated derivations of the GR rate[18,19(a)] extend its validity to long times under conditions which promote simple exponential decay. The question of whether the nonequilibrium golden rule can correctly predict the full history of the electronic population evolution can only be answered by comparing nonequilibrium golden rule results to exact results for appropriate model problems. Since our development of the formula relies strongly on the presence of a multidimensional "bath" of nuclear coordinates, there are not many systems (featuring both a large environment of bath coordinates *and* curve crossing between two potential surfaces) for which exact results can be obtained.

Fortunately, a model for electron transfer, due to Garg, Onuchic, and Ambegaokar (GOA),[20] which is of spin–boson type, is very useful for our purposes in two ways. First, it is multidimensional in nuclear space, and second, it can be solved essentially exactly. We note that Garg *et al.* were interested in initial conditions corresponding to equilibrium preparation in the donor electronic state. Here we study cases of nonequilibrium initial preparation as well. We have succeeded, by explicit enumeration of the spin configurations that arise in the path integral (PI) representation of the dynamics of the spin–boson model, to converge the quantum dynamics of substantial portions of the electronic decay curves over a range of initial conditions and potential parameters. These results have been compared to the predictions of the nonequilibrium golden rule formula, with good agreement obtained in all cases studied. In the rest of this paper, we present our formulation and the results of our numerical studies according to the following outline.

In Sec. II, the NGR formalism is presented. In Sec. III, the GOA model is introduced and our procedure for modifying it in the case of nonequilibrium preparation on the initially populated (donor) potential surface is described. Then, in Sec. IV, numerically exact results for this model, obtained by explicit spin-path enumeration, are compared to approximate results obtained from the NGR formula. The paper concludes with a discussion in Sec. V in which the strengths and weaknesses of the NGR method are summarized and possible directions for future work suggested.

II. A NONEQUILIBRIUM GOLDEN RULE FORMULA

A. The time dependent rate constant

Consider two nuclear Hamiltonians $\hat{h}_b$ and $\hat{h}_d$ that describe the motion on different electronic potential surfaces V_b and V_d and which interact via nonadiabatic or other coupling terms.[21] To be concrete, let $\hat{h}_b=\hat{T}+V_b(\hat{x})$ and $\hat{h}_d=\hat{T}+V_d(\hat{x})$, where $\hat{T}$ is the nuclear kinetic energy operator. The dimensionality of the nuclear coordinate space, the coordinate system employed, and the functional form of $V_{b,d}$ are arbitrary. (In this section we employ a one dimensional description of the nuclear motion for notational simplicity. To treat the multidimensional case, regard the position and momentum variables as vector quantities, with one component for each Cartesian degree of freedom.) The subscripts "b" and "d" stand for "bright" and "dark," a designation again adopted for concreteness.[22] In a common scenario, a molecule in its electronic ground state is optically excited to a bright electronic state and its subsequent evolution is affected by radiationless transition induced by nonadiabatic coupling to a second electronic state nearby in energy, but radiatively dark, i.e., not coupled radiatively to the ground state. The nonadiabatic coupling function is denoted by $g(\hat{x},\hat{p})$.

The specific question asked is "Given preparation of an initial nuclear wave packet $\phi_0(x)$ on the bright surface V_b, what is the probability that the molecule remains on the bright surface at a later time t, or, equivalently, what is the time dependence of the electronic population of the bright state?" Let us term this quantity $P_b(t)$. It is related to nuclear dynamics on the coupled surfaces V_b and V_d. The molecular Hamiltonian operator that governs this motion is

$$\hat{H}=|b\rangle\langle b|\hat{h}_b+|d\rangle\langle d|\hat{h}_d+\hat{g}(|b\rangle\langle d|+|d\rangle\langle b|). \tag{2.1}$$

Here $|b\rangle$ and $|d\rangle$ are the bright and dark electronic states, respectively, which are assumed independent of nuclear coordinates.

Downloaded 17 Mar 2004 to 132.66.16.34. Redistribution subject to AIP license or copyright, see http://jcp.aip.org/jcp/copyright.jsp

In terms of the Hamiltonian (2.1), the bright state electronic population is, irrespective of the rovibrational state of the nuclear motion,

$$P_b(t)=\langle\phi_0|\langle b|e^{i\hat{H}t}|b\rangle\langle b|e^{-i\hat{H}t}|b\rangle|\phi_0\rangle. \tag{2.2}$$

Note that we set $\hbar=1$ throughout. Furthermore, for simplicity, we concentrate on the case that the nuclear coordinates are prepared at $t=0$ in a pure state, described by a wave function $\phi_0(x)$. Our results can easily be adapted to the case where the nuclear coordinates are prepared in a mixed state described by an appropriate density matrix.

We calculate $P_b(t)$ to lowest nontrivial order in perturbation theory. This perturbation expansion is predicated on the smallness of the nonadiabatic coupling strength, i.e., we decompose $\hat{H}=\hat{H}_0+\hat{V}_I$ with

$$\hat{H}_0=|b\rangle\langle b|\hat{h}_b+|d\rangle\langle d|\hat{h}_d \tag{2.2a}$$

and

$$\hat{V}_I=\hat{g}(|b\rangle\langle d|+|d\rangle\langle b|). \tag{2.2b}$$

Hence the Heisenberg operator $\hat{V}_I(t) = e^{i\hat{H}_0t}\hat{V}_Ie^{-i\hat{H}_0t}$ is given explicitly by

$$\hat{V}_I(t)=e^{i\hat{h}_bt}\hat{g}e^{-i\hat{h}_dt}|b\rangle\langle d|+e^{i\hat{h}_dt}\hat{g}e^{-i\hat{h}_bt}|d\rangle\langle b|. \tag{2.3}$$

Then the propagator $e^{-i\hat{H}t}$ can be written as $e^{-i\hat{H}t} = e^{-i\hat{H}_0t}\hat{U}_I(t)$, where the interaction picture evolution operator $\hat{U}_I(t)$ can be computed order by order in perturbation theory according to

$$\hat{U}_I(t)=1-i\int_0^t dt'\hat{V}_I(t')dt'-\int_0^t dt'\int_0^{t'}dt''\hat{V}_I(t')\hat{V}_I(t'') + \cdots . \tag{2.4}$$

$P_b(t)$ can be written directly in terms of $\hat{U}_I(t)$,

$$P_b(t)=\langle\phi_0|\langle b|\hat{U}_I(t)^\dagger|b\rangle\langle b|\hat{U}_I(t)|b\rangle|\phi_0\rangle. \tag{2.5}$$

Thus, the critical quantity is $\langle b|\hat{U}_I(t)|b\rangle$, which is an operator on nuclear coordinates. It is obtained (perturbatively) by taking the appropriate electronic matrix element of Eq. (2.4)

$$\langle b|\hat{U}_I(t)|b\rangle=1-\int_0^t dt'\int_0^{t'}dt''e^{i\hat{h}_bt'}\hat{g} \times\exp[-i\hat{h}_d(t'-t'')]\hat{g}e^{-i\hat{h}_bt''}+O(g^4). \tag{2.6}$$

Inserting this expression into Eq. (2.5) leads to an explicit evaluation of the short-time evolution of the electronic population

$$P_b(t)=1-2\ \mathrm{Re}\int_0^t dt'\int_0^{t'}dt''\langle\phi_0|e^{i\hat{h}_bt'}\hat{g} \times\exp[-i\hat{h}_d(t'-t'')]\hat{g}e^{-i\hat{h}_bt''}|\phi_0\rangle+O(g^4). \tag{2.7}$$

It is convenient to define

$$k(t)\equiv 2\ \mathrm{Re}\int_0^t dt'\langle\phi_0|e^{i\hat{h}_bt'}\hat{g} \times\exp[-i\hat{h}_d(t-t')]\hat{g}e^{-i\hat{h}_bt'}|\phi_0\rangle; \tag{2.8}$$

$k(t)$ can be interpreted as a time dependent rate constant in the following manner:

$$P_b(t)=1-\int_0^t dt'k(t')+\cdots \tag{2.9a}$$

$$\cong\exp\left[-\int_0^t dt'k(t')\right]. \tag{2.9b}$$

The exponentiation step in Eq. (2.9b) can be justified, under certain conditions, for the special case where $|\phi_0\rangle$ is an eigenstate of $\hat{h}_b$. One manifestation of these conditions is "one-way flow," i.e., the probability amplitude that leaks onto V_d does not find its way back to V_b. It is intuitively expected and we make the ansatz that Eq. (2.9b) holds also for general nonstationary $|\phi_0\rangle$, provided that the conditions for one-way flow are satisfied. Of course, this expectation remains to be checked; a careful attempt to do so is presented in Secs. III and IV.

An alternative way to write $k(t)$ is

$$k(t)=2\ \mathrm{Re}\int_0^t d\tau\ tr[\hat{\rho}(t)\hat{g}e^{-i\hat{h}_d\tau}\hat{g}e^{i\hat{h}_b\tau}] \tag{2.10a}$$

$$=2\ \mathrm{Re}\int_0^t d\tau\langle\phi_0(t)|\hat{g}e^{-i\hat{h}_d\tau}\hat{g}e^{i\hat{h}_b\tau}|\phi_0(t)\rangle. \tag{2.10b}$$

Here $\hat{\rho}(t)=|\phi_0(t)\rangle\langle\phi_0(t)|$, with $|\phi_0(t)\rangle = e^{-i\hat{h}_bt}|\phi_0\rangle$. That is, $|\phi_0(t)\rangle$ is the wave packet obtained by propagating $|\phi_0\rangle$ on V_b or, equivalently, $\hat{\rho}(t)$ is the density matrix associated with the evolution of initial density matrix $|\phi_0\rangle\langle\phi_0|$ according to $\hat{h}_b$. The form of $k(t)$ given in Eq. (2.10) has some interpretive and computational advantages.

In the case where $|\phi_0\rangle$ is an eigenstate of $\hat{h}_b$, say $|\phi_j^{(b)}\rangle$, then provided certain conditions are satisfied, after the transient time τ_c, $k(t)$ attains a time independent value given by the standard GR result

$$k_j=2\ \mathrm{Re}\int_0^\infty d\tau\langle\phi_j^{(b)}|\hat{g}e^{-i\hat{h}_d\tau}ge^{i\hat{h}_b\tau}|\phi_j^{(b)}\rangle. \tag{2.11}$$

τ_c is the time scale on which the integrand in Eq. (2.11) decays to zero, and the conditions for validity of Eq. (2.11) are essentially those that ensure that such relaxation to zero indeed occurs on a short enough time scale. Neglecting deviations at short times, this implies simple exponential decay, i.e., $P_b(t) = e^{-k_jt}$, with the rate constant given in Eq. (2.11). The purpose of the present work is, again, to generalize our understanding to the case of out-of-equilibrium initial preparation. By following a similar line of reasoning that leads to Eq. (2.11), we may assert that provided that $t\gg\tau_c$, then the generalization of Eq. (2.11) to the nonequilibrium case is

$$k(t)=2\ \mathrm{Re}\int_0^\infty d\tau\langle\phi_0(t)|\hat{g}e^{-i\hat{h}_d\tau}\hat{g}e^{i\hat{h}_b\tau}|\phi_0(t)\rangle. \tag{2.12}$$

Equation (2.12) provides an elegant interpretation of the time dependent rate constant as the rate associated with the relaxation of the instantaneous wave function $|\phi_0(t)\rangle$. If, in an interacting many body system, the relaxation of $\phi_0(t)$ leads

Downloaded 17 Mar 2004 to 132.66.16.34. Redistribution subject to AIP license or copyright, see http://jcp.aip.org/jcp/copyright.jsp

to a thermal distribution on the bright surface, Eq. (2.12) will again become the standard GR expression for times t that exceed the thermal relaxation time.

B. Semiclassical evaluation of the rate constant

The expressions for $k(t)$ in Eqs. (2.9), (2.10), and (2.12) rely on sequential nuclear wave packet propagations on bright and dark potential energy surfaces. For interacting many-body systems, exact evaluation is not feasible. However, several semiclassical evaluation schemes appear viable. First, if the initial wave packet $|\phi_0\rangle$ can be expressed as a linear combination of Gaussian wave packets, then Gaussian wave packet dynamics at either the "thawed" or "frozen Gaussian" level[23] can be carried out even in condensed phase systems. Indeed, Neria and Nitzan have recently demonstrated the applicability of such techniques to the case of standard golden rule rates, i.e., Eq. (2.11).[11] There is no obvious reason why the same procedures should not work as well in the case of nonequilibrium initial state preparation covered by Eqs. (2.9b) and (2.10).

Another kind of semiclassical procedure is suggested by the argument presented above that the integrand of Eq. (2.10) decays rapidly as a function of τ. For small τ, it is legitimate[10] to replace $e^{-ih_d\tau}\hat{g}e^{ih_b\tau}\rightarrow\hat{g}e^{-i\Delta V(\hat{x})\tau}$, with $\Delta V(\hat{x})\equiv V_d(\hat{x})-V_b(\hat{x})$. This implies the approximate formula $k(t)=\int_0^t d\tau\, C(\tau,t)$ with

$$C(\tau,t)=2\ \mathrm{Re}\int dx\ P_0(x,t)g^2(x)e^{-i\Delta V(x)\tau} \tag{2.13a}$$

and

$$P_0(x,t)=|\phi_0(x,t)|^2. \tag{2.13b}$$

In Eqs. (2.13), spatial integrals are over all nuclear coordinate space. Also, we have assumed the nonadiabatic coupling function is not a function of momentum in obtaining this form. The advantage of this result is that it can be evaluated numerically using classical or quantum molecular dynamics simulation to evaluate $P_0(x,t)$. We note that in the semiclassical spirit of the approximation, it is expected that Wigner distributions can be used to define a phase space representation of $|\phi_0\rangle\langle\phi_0|$, and classical mechanics used to propagate it.

C. Classical Franck–Condon approximation to $k(t)$

If we approximate the time kernel which appears in Eq. (2.10) by $C(\tau,t)$ given in Eq. (2.13), and simultaneously extend the upper limit of the time integration to infinity [cf. Eq. (2.12)], we obtain the "classical Franck–Condon" type expression

$$k(t)\approx 2\pi\int dx\ P_0(x,t)g^2(x)\delta[\Delta V(x)], \tag{2.14}$$

where "δ" is the Dirac delta function. In this quasiclassical limit, the only part of the coordinate space that contributes to the nonadiabatic transition rate is the crossing seam between V_b and V_d. Points along the seam are weighted by the instantaneous probability of the system to be at the seam (and also, in a milder way, by the gradient of the potential surface difference along the seam). This formula shows clearly the modulation of the time dependent rate constant as the wave packet enters and leaves the crossing region, as may have been expected on intuitive grounds and as has been observed recently in the photodissociation of NaI and NaBr by Zewail and co-workers.[7(b)] Also, as discussed above, it shows the approach to the thermally relaxed rate as $P_0(x,t)$ relaxes to thermal equilibrium. Thus the time evolution of the electronic population is governed by leakage to the dark surface and (vibrational) relaxation on the bright surface.

It is important to appreciate that although we have chosen to describe the curve-crossing scenario in the language of radiationless transition theory, the same scenario and same analysis applies to a variety of phenomena. Electron transfer reactions are a particularly popular case in point, where bright and dark states become "donor" and "acceptor" states, respectively. In the next section, we study a multimode model of electron transfer which can be addressed directly by the NGR formula.

III. A SPIN–BOSON MODEL OF "INNER-SPHERE" ELECTRON TRANSFER IN THE CASE OF NONEQUILIBRIUM PREPARATION OF THE DONOR STATE

Many electron transfer reactions are thought to proceed via the so-called "inner-sphere" mechanism. Namely, one (or a few) degrees of freedom are directly coupled to the electron transfer process. These "primary" or "reaction" coordinates are coupled to the environment of "secondary" or "bath" coordinates. The latter thus affect the electron transfer process indirectly, put possibly in a significant way.

Garg *et al.*[20] have modeled the reaction coordinate dynamics via two harmonic potential wells—one for the donor state and one for the acceptor state. The two wells are characterized by the same frequency and are shifted with respect to the locations of the minima and their energetic origins. The bath is modeled as a collection of uncoupled harmonic oscillators, each of which is coupled bilinearly to the reaction coordinate. Such a description of the environment and its coupling to the reaction coordinate has been very popular in recent years.[19] It results in relatively tractable reduced dynamics of the reaction coordinate at both classical and quantum levels. Moreover, by choosing the frequencies and bilinear coupling strengths of the bath oscillators appropriately, a variety of condensed phase environments can be mimicked.

The Hamiltonian corresponding to this model can be written as

$$\hat{H}=\hat{h}_+|+\rangle\langle+|+\hat{h}_-|-\rangle\langle-|+\tfrac{1}{2}\Delta_0(|+\rangle\langle-|+|-\rangle\langle+|). \tag{3.1}$$

Here $|+\rangle$ and $|-\rangle$ are the diabatic electronic states corresponding to the donor and acceptor electronic configurations, respectively. The nuclear coordinate Hamiltonians $\hat{h}_\pm$ are specified as

$$\hat{h}_\pm=\frac{\hat{p}_y^2}{2}+V_\pm(\hat{y})+\sum_\alpha\left[\frac{\hat{p}_\alpha^2}{2}+\frac{1}{2}\omega_\alpha^2\left(\hat{x}_\alpha+\frac{c_\alpha\hat{y}}{\omega_\alpha^2}\right)^2\right]. \tag{3.2}$$

Downloaded 17 Mar 2004 to 132.66.16.34. Redistribution subject to AIP license or copyright, see http://jcp.aip.org/jcp/copyright.jsp

We have labeled the reaction coordinate as y, and the reaction coordinate potentials appropriate to donor and acceptor electronic state are labeled as $V_{\pm}(y)$. (Our notation follows Garg *et al.* throughout, except that for simplicity and without any loss of generality, we have set $\hbar$ and all masses to unity.) In the simplest version of the GOA model (described above),

$$V_{\pm}(y)=\tfrac{1}{2}\Omega^2(y\pm y_0)^2\pm\tfrac{1}{2}\epsilon_0. \tag{3.3}$$

These reaction coordinate potentials represent two harmonic oscillator wells with the same angular frequency Ω whose equilibrium positions are separated by a distance $2y_0$ and whose minima differ in energy by ϵ_0. There are two very appealing features about the ET Hamiltonian defined in Eqs. (3.1)–(3.3). First, irrespective of any particular model for $V_{\pm}(y)$, the classical mechanics of the system coordinate (moving on one of the diabatic potential energy surfaces) can be described via a generalized Langevin equation in which the memory friction kernel is determined by the frequency distribution of the bath oscillators and by the bilinear coupling coefficients that connect them to the system coordinate (see below). Second, if the functional form given in Eq. (3.3) is adopted for $V_{\pm}$, the ET Hamiltonian is then of canonical spin–boson form. Garg *et al.* utilized this mapping to perform elegant but approximate analysis of the quantum dynamics of the model using techniques developed in the macroscopic tunneling literature.[19(a)] Our approach to the computation of the necessary quantum dynamics will be somewhat different. We have found that it is possible to explicitly enumerate enough spin configurations in the path integral representation of the spin–boson (SB) model to obtain numerical results of desired accuracy.

Regardless of the manner in which the quantum dynamics calculations are performed, there remains the issue of choosing the parameters in the Hamiltonian and the initially prepared nuclear state on the donor surface. Here we will extend the line of reasoning adopted by Garg *et al.* to construct the simplest model that has the necessary features. We consider nuclear motion on the initially occupied donor potential surface. If one chooses the bath oscillator frequencies ω_α and the system–bath coupling coefficients c_α according to the spectral density

$$J_0(\omega)=\frac{\pi}{2}\sum_\alpha\frac{c_\alpha^2}{\omega_\alpha}\,\delta(\omega-\omega_\alpha)=\eta\omega\,\exp(-\omega/\Lambda), \tag{3.4}$$

and the initial displacements $x_\alpha^{(0)}$ of the bath coordinates are tuned to the initial displacement $y^{(0)}$ of the reaction coordinate as $x_\alpha^{(0)}=-c_\alpha y^{(0)}/\omega_\alpha^2$, then the classical dynamics of the reaction coordinate obeys the simple (zero-temperature) Langevin equation[24]

$$d^2y/dt^2+dV_+(y)/dy+\eta dy/dt=0. \tag{3.5}$$

[The factor $\exp(-\omega/\Lambda)$ in Eq. (3.4) ensures a smooth cutoff of the spectral density at higher frequency. As $\Lambda\to\infty$, the Λ-independent Langevin equation (3.5) is obtained.] Since the donor surface is of harmonic oscillator type, the quantum dynamics of a Gaussian wave packet placed on the donor surface at $t=0$ will reflect the classical evolution given by Eq. (3.5). More specifically, the center of the position space Gaussian, i.e., the center of the reduced probability distribution in the reaction coordinate, will relax in exactly the manner prescribed in Eq. (3.5).

The construction of the details of the system–bath coupling scheme just sketched follows the reasoning of Garg *et al.* closely. Their work only considered the equilibrium case $y^{(0)}=y_0$, and thus explicit relaxation of the reduced probability distribution of the reaction coordinate was not studied. The new feature that we have to contend with is starting the reaction coordinate out of equilibrium, i.e., $y^{(0)}\neq y_0$. Our inclusion of this feature introduces one additional complication, namely, the need to prescribe the remaining features of the initially prepared wave packet on the donor surface.

In the GOA model, the appropriate initial nuclear state at zero temperature is simply a product of Gaussian wave packets that represent the vibrational ground state of each of the normal modes of the full system–bath potential energy function associated with the donor electronic state. This state corresponds to equilibrium preparation on the donor surface at zero temperature and, moreover, is easy to process within the standard procedures utilized to compute real-time dynamics of spin–boson models.

In our generalization, the initial nuclear state is prescribed by a product of one-dimensional coherent state wave packets in the normal modes of the donor potential surface. Each coherent state is simply a displaced version of the ground state Gaussian wave packet for that mode, with its center in position space taken as the appropriate normal mode displacement that will produce the Cartesian displacements $y^{(0)}\neq y_0$ and $x_\alpha=-c_\alpha y^{(0)}/\omega_\alpha^2$ introduced above.

The model just described has the following desirable properties: It mimics the properties of an interacting many-body system well enough to exhibit vibrational relaxation of the reaction coordinate as it dissipates its initial energy into its environment. Because the reaction coordinate is directly coupled to the electronic degrees of freedom of the system, the model enables study of the joint contributions of vibrational relaxation and electron transfer to the overall decay of the donor state population. Finally, the model is of spin–boson form. This means that the problem can be mapped onto one of enumerating configurations of a linear chain of Ising spins. Although previous work that has used this formulation of the SB model to compute real-time dynamical signatures has assumed preparation in vibrational eigenstates (or the associated thermal density operator[19,20,25]), the same explicit enumeration procedure can be utilized to study the evolution of the displaced initial state that is relevant in our scenario.

We stress that the spin–boson model of nonequilibrium inner sphere ET which has been constructed is not without deficiencies. The spectral densities invoked mimic relaxation of the reaction coordinate via dissipative coupling to an environmental bath, but we have no evidence that the relaxation of any particular molecular ET system is governed specifically by the Langevin equation (3.5). In addition, the details of the initial nonequilibrium nuclear coordinate wave packet are chosen largely for convenience. The need to shift the center of the wave packet along the reaction coordinate

Downloaded 17 Mar 2004 to 132.66.16.34. Redistribution subject to AIP license or copyright, see http://jcp.aip.org/jcp/copyright.jsp

away from the equilibrium position along that coordinate is self-evident, but other features such as the widths of the initial wave packet in each direction of nuclear coordinate space depend intimately on the nature of preparation of the initial state, an issue which is beyond the scope of the present study. Moreover, the nuclear motion on the bright surface cannot truly exhibit relaxation to equilibrium, since the bright surface potential energy function is quadratic in the nuclear coordinates. Hence the evolution $\hat{\rho}(t)\rightarrow\hat{\rho}_\beta$, where $\hat{\rho}_\beta$ is the thermal equilibrium density matrix associated with $\hat{h}_b$, does *not* occur in this model. Fortunately, for the spectral densities adopted in this work (full details are given below), the critical time kernels do have the property that for long times t,

$$\langle\phi_0(t)|\hat{g}e^{-i\hat{h}_d\tau}\hat{g}e^{i\hat{h}_b\tau}|\phi_0(t)\rangle\rightarrow\langle\phi_0^{(b)}|\hat{g}e^{-i\hat{h}_d\tau}\hat{g}e^{i\hat{h}_b\tau}|\phi_0^{(b)}\rangle. \tag{3.6}$$

Hence the time dependent rate constant $k(t)$ relaxes at long times to an asymptotic value given by the standard GR in our model calculations.

Another type of limitation of the present model, in which the coupling between the reaction coordinate and the bath is linear in the reaction coordinate, is that it underestimates the role of vibrational dephasing in the molecular relaxation process. It does not account for dephasing processes not directly associated with population relaxation (i.e., "proper dephasing"). From the point of view of the present calculation, this does not raise any difficulty because, as pointed out in Sec. I, in the limit of fast dephasing, the relaxation can be described by a standard master equation in the space of vibrational levels of the initial electronic state with each level assigned a decay rate given by the standard golden rule. Here we focus on the opposite limit. In the next section, we provide specific parameter choices, details of computation, and results for electron transfer in the case of preparation in a nonequilibrium nuclear coordinate state of the donor potential surface.

IV. COMPUTATIONAL DETAILS AND RESULTS

The electron transfer Hamiltonian used in our numerical study is given in Eqs. (3.1)–(3.3). The displacements which describe the shift of the dark state from the bright state are specified by the spectral density $J_0(\omega)$ given by Eq. (3.4). The nuclear coordinates y and $\{x_\alpha\}$ can be exchanged for linear combinations $\{\tilde{x}_\beta\}$ corresponding to the normal modes of the quadratic potential indicated in Eqs. (3.2) and (3.3) (i.e., the coordinates in which the associated force constant matrix is diagonal). Expressed in terms of normal mode coordinates, the ET Hamiltonian reads

$$\hat{H}_{\rm ET}=\frac{\Delta_0}{2}\boldsymbol{\sigma}_{\rm x}+y_0\boldsymbol{\sigma}_{\rm z}\sum_\beta\tilde{c}_\beta\tilde{x}_\beta+\sum_\beta\left(\frac{\tilde{p}_\beta^2}{2}+\frac{1}{2}\tilde{\omega}_\beta^2\tilde{x}_\beta^2+\frac{\tilde{c}_\beta^2y_0^2}{2\tilde{\omega}_\beta^2}\right)\mathbf{1}+\sigma_{\rm z}\frac{\epsilon_0}{2}, \tag{4.1}$$

where $\tilde{x}_\beta$ are the normal modes, and $\tilde{p}_\beta$ and $\tilde{\omega}_\beta$ are the corresponding canonical momenta and frequencies, respectively. (If there are N bath oscillators x_α, then there are of course $N+1$ normal mode coordinates $\tilde{x}_\beta$. Also, for notational simplicity, circumflexes on the position and momentum operators associated with the normal mode coordinates are suppressed in this section.) $\hat{H}_{\rm ET}$ is now in the form of a spin-$\frac{1}{2}$ system (represented by 2×2 Pauli spin matrices $\boldsymbol{\sigma}_{\rm x}$ and $\boldsymbol{\sigma}_{\rm z}$ and the 2×2 unit matrix) coupled to a set of mutually independent harmonic oscillators. The dynamics of the composite spin–boson system is amenable to calculation via exact path integral methods as well as the (approximate) nonequilibrium golden rule method introduced here. As shown by Garg *et al.* the coefficients $\tilde{c}_\beta$ and the frequencies $\tilde{\omega}_\beta$ that correspond to $J_0(\omega)$ in Eq. (3.4) are prescribed by the spectral density

$$J_{\rm eff}(\omega)=\frac{\pi}{2}\sum_\beta\frac{\tilde{c}_\beta^2}{\tilde{\omega}_\beta}\delta(\omega-\tilde{\omega}_\beta)=\frac{\eta\omega\Omega^4}{(\Omega^2-\omega^2)^2+\omega^2\eta^2}. \tag{4.2}$$

For the nonequilibrium model, the initial wave packet is not in thermal equilibrium on the + surface. As was noted in Sec. III, if the initial displacement of the reaction coordinate is $y^{(0)}$, then the initial displacement of the bath coordinates $x_\alpha^{(0)}$ must be taken as $x_\alpha^{(0)}=-c_\alpha y^{(0)}/\omega_\alpha^2$, in order for the reaction coordinate to obey the simple zero-temperature Langevin equation dynamics given in Eq. (3.5)

If the transformation matrix between the local modes and the normal modes is denoted by $\mathbf{T}$ (i.e., the columns of $\mathbf{T}$ are the unit normed eigenvectors of the force constant matrix associated with the coupled reaction coordinate-bath potential energy surface), then

$$\mathbf{T}^t\begin{pmatrix}1\\-\frac{c_1}{\omega_1^2}\\\vdots\\-\frac{c_\alpha}{\omega_\alpha^2}\\\vdots\end{pmatrix}=\begin{pmatrix}\frac{\tilde{c}_1}{\tilde{\omega}_1^2}\\\vdots\\\frac{\tilde{c}_\beta}{\tilde{\omega}_\beta^2}\\\vdots\end{pmatrix}. \tag{4.3}$$

The initial displacements $y^{(0)}$ and $x_\alpha^{(0)}=-c_\alpha y^{(0)}/\omega_\alpha^2$ on the + (donor) potential energy surface correspond to normal mode displacements $\tilde{x}_\beta^{(0)}$ given by

$$\begin{pmatrix}\tilde{x}_1^{(0)}\\\vdots\\\tilde{x}_\beta^{(0)}\\\vdots\end{pmatrix}=y^{(0)}\mathbf{T}^t\begin{pmatrix}1\\-\frac{c_1}{\omega_1^2}\\\vdots\\-\frac{c_\alpha}{\omega_\alpha^2}\\\vdots\end{pmatrix}=y^{(0)}\begin{pmatrix}\frac{\tilde{c}_1}{\tilde{\omega}_1^2}\\\vdots\\\frac{\tilde{c}_\beta}{\tilde{\omega}_\beta^2}\\\vdots\end{pmatrix}. \tag{4.4}$$

Thus the initial displacements on the + surface are proportional to $\tilde{c}_\beta/\tilde{\omega}_\beta^2$, where the parameters $\tilde{c}_\beta$ are chosen according to $J_{\rm eff}$ given in Eq. (4.2). More precisely, the displacement of the βth normal mode wave packet from the equilibrium position of this mode on the + surface can therefore be written as

$$(y^{(0)}+y_0)\frac{\tilde{c}_\beta}{\tilde{\omega}_\beta^2}. \tag{4.5}$$

Downloaded 17 Mar 2004 to 132.66.16.34. Redistribution subject to AIP license or copyright, see http://jcp.aip.org/jcp/copyright.jsp

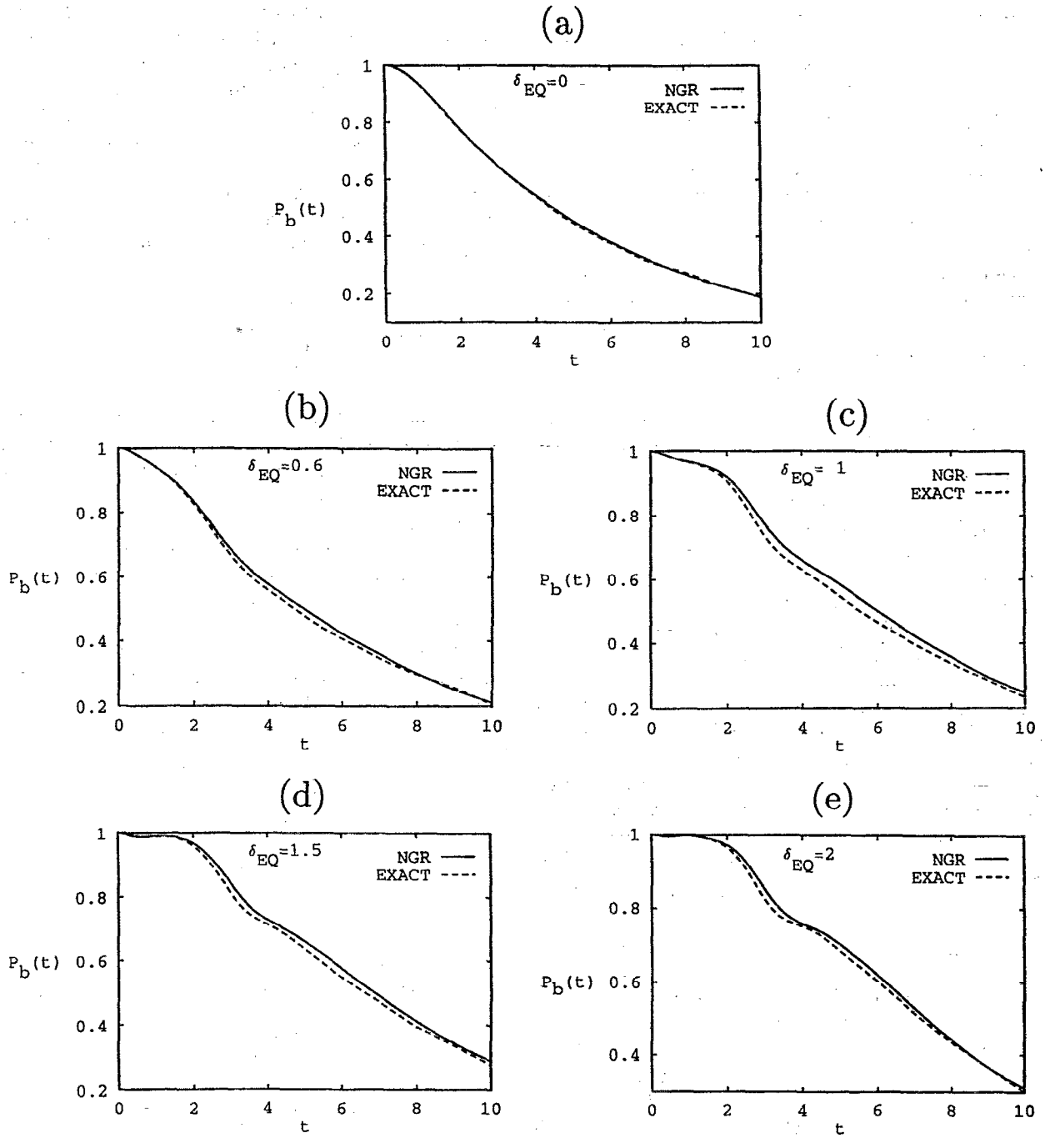

FIG. 1. $P_b(t)$ obtained from the nonequilibrium golden rule formula, indicated by a solid line, is compared with exact results (indicated by a dashed line) for the "barrierless crossing" electron transfer (ET) Hamiltonian discussed in Sec. IV. The value of the nonadiabatic coupling strength is Δ_0=0.6. In (a), the wave packet is started at the equilibrium position of the + (donor) surface, i.e., $y^{(0)}=-y_0$; in (b)–(e), the initial wave packet is started out of equilibrium. The extent of the initial displacement $\delta_{eq}\equiv-(y^{(0)}+y_0)$ from equilibrium is indicated.

The system which has been studied consists of a reaction coordinate y with a frequency of oscillation $\Omega=1$. As mentioned above, the mass is taken as unity, and so is the parameter y_0 which determines the horizontal displacement of the minima corresponding to $V_{\pm}$. The reaction coordinate is coupled bilinearly to a bath of oscillators of unit mass, as described in the GOA Hamiltonian [cf. Eq. (3.2)]. The coupling coefficients $\tilde{c}_\beta$ are chosen according to $J_{\text{eff}}(\omega)$, using a value for the friction constant of $\eta=1$. The procedure by which the normal mode frequencies, their equilibrium positions, and the relevant initial (displaced) wave packet states are chosen may be summarized as follows: mode frequencies are evenly distributed between zero and a cut-off frequency much larger than Ω. For each frequency $\tilde{\omega}_\beta$, the parameter

Downloaded 17 Mar 2004 to 132.66.16.34. Redistribution subject to AIP license or copyright, see http://jcp.aip.org/jcp/copyright.jsp

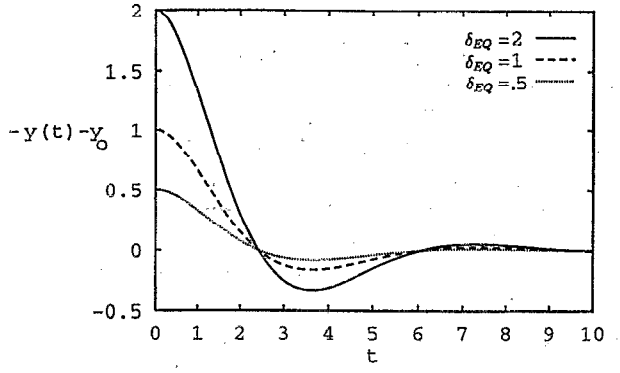

FIG. 2. Classical dynamics of the system coordinate $y(t)$ on the + electronic surface. Trajectories are shown for three initial displacements from equilibrium. Values of δ_{eq} are indicated on the figure.

$\tilde{c}_\beta$ is chosen according to Eq. (4.2), and the displacement of the mode from equilibrium is given by Eq. (4.5). As indicated above, the width of the initial wave packet associated with normal mode coordinate β is the same as for the vibrational ground state of a simple harmonic oscillator having unit mass and angular frequency $\tilde{\omega}_\beta$.

We have examined situations corresponding to several values of the bias energy ϵ. In the first example to be presented, the minimum of the $-$ surface is lower in energy by an amount $\epsilon_0=\Sigma_\beta 2\tilde{c}_\beta^2/\tilde{\omega}_\beta^2$ than that of the + surface, so that the $-$ surface intersects the + surface at the minimum $y=-y_0$ of the latter. This arrangement promotes rapid leakage of the wave packet onto the dark surface (assuming that the initial nuclear wave packet is prepared in or quickly approaches the equilibrium region of the donor surface). In the ET literature, it is referred to as the case of "activationless" transfer. The nonadiabatic coupling parameter Δ_0 is set to 0.6. Results for a series of model systems in which the initial wave packet is gradually shifted further from the thermal equilibration position are shown in Fig. 1. In all cases, the initial displacement of the wave packet from equilibrium $-(y^{(0)}+y_0)\equiv\delta_{eq}$ is indicated.

In Fig. 1, $P_b(t)$ obtained via the nonequilibrium golden rule formula [Eqs. (2.8) and (2.9b)] is compared with the result obtained by the exact spin enumeration procedure. Panels (1a)–(1e) show results for increasing values of δ_{eq}. The details of the exact calculation of $P_b(t)$ are outlined in the Appendix. In all calculations, a discrete set of bath oscillators was used and the number of oscillators was increased until convergence over the desired time period was achieved. In general, this required approximately 200 oscillators.

Figure 1(a) depicts the case of equilibrium preparation, i.e., $y^{(0)}=-y_0$. This curve shows the familiar behavior associated with the standard golden rule. At short times, $P_b(t)$ decays quadratically with time, but at longer times, exponential decay sets in. Panels 1(b)–1(e) show results for increasing initial displacement of the reaction coordinate. The first noticable effect of such a displacement is a delay in the initial probability leakage due to the fact that the initial nuclear coordinates have a very small probability to be at the crossing seam (which goes through the equilibrium position of the donor surface for this system). As the initial state begins to evolve on the bright surface, it "rolls down" to the bottom of the donor surface and nonadiabatic transfer to the acceptor surface can occur. As the initial dispacement is increased further, a succession of plateaus and dips develop in $P_b(t)$. These reflect successive seam crossings [manifested in dips in $P_b(t)$] and departures from the seam region [manifested as plateaus in $P_b(t)$]. Because the reaction coordinate dynamics is coupled to a zero temperature harmonic bath, the center of the nuclear probability density along the reaction coordinate coordinate damps to y_0, which results in an asymptotically time-independent rate constant, i.e., simple exponential decay of $P_b(t)$.

This interpretation of the dynamics is supported by Fig. 2, which shows the classical motion for the reaction coordinate on the + electronic surface, computed from the Langevin equation (3.5). As noted above, increasing the displacement of the y coordinate from the equilibrium position results in slower initial decay of $P_b(t)$. Since the intersection of + and $-$ surfaces occurs at the bottom of the + surface well, transfer to the dark surface is most efficient when the wave packet is in this region. According to the classical decay dynamics of $y(t)$, the larger the initial displacements are from the minimum in the potential energy surface, the further the system is from its equilibrium position at shorter times. In a quantum mechanical scenario, this may be interpreted as the center of the wave packet being further displaced from the crossing point and hence less efficient transfer at shorter times.

Further insight into the dynamics is obtained by plotting $\ln[P_b(t)]$ vs t for the curves obtained in Figs. 1(a)–1(e). This is done in Fig. 3. At sufficiently long times, all the curves become straight lines with nearly the same slope. This reflects expectations set forth in Sec. II above. The time dependent rate constant $k(t)$ {the negative of the slope of $\ln[P_b(t)]$} directly mirrors the evolution on the donor surface of the initially prepared nuclear wave packet, as indicated in Eq. (2.12). After a long enough time, for the donor surface used in the present study, the reduction indicated in

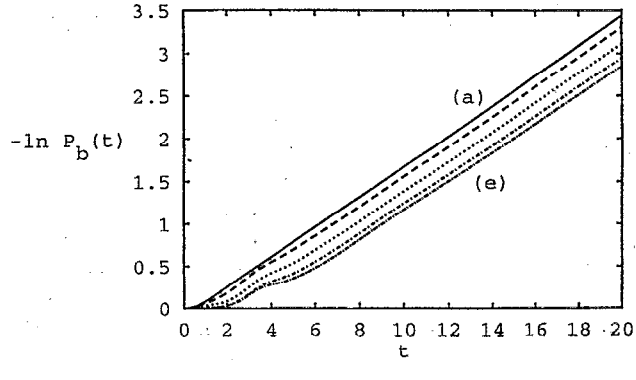

FIG. 3. $P_b(t)$ vs time for the ET system considered in Fig. 1. Data are taken from NGR computations. All curves have essentially the same asymptotic slope, consistent with the standard golden rule rate. The curves corresponding to the initial displacements in Fig. 1(a) and 1(e) are indicated on the graph. The curves for Figs. 1(b)–1(d) progress smoothly between these two cases.

Downloaded 17 Mar 2004 to 132.66.16.34. Redistribution subject to AIP license or copyright, see http://jcp.aip.org/jcp/copyright.jsp

Eq. (3.6) occurs. We expect this to be the case in more complicated condensed phase systems as well for reasons outlined in the discussion of the classical Franck–Condon approximation to $k(t)$ above.

For the range of displacements from equilibrium considered in Fig. 1, the NGR provides a good approximation to the exact solution, up to times where less than about 30% of the initial population remains on the + surface. It should be noted that the exact calculations of the population decay, using the spin enumeration procedure described in the Appendix, require enough spins to achieve convergence over the time period of interest. The number needed depends in part on the values of the parameters that appear in the ET Hamiltonian (4.1), and also on the time interval of interest. For the systems considered in Fig. 1, it was found that for $t \leqslant 8$, about 14 spins, or 2^{14} spin configurations were sufficient, while for the long time tails $8 \leqslant t \leqslant 10$, considerably more configurations were required for convergence, typically 2^{18}–2^{26}.

The case of "barrierless crossing" is special, since it is defined by the condition that the diabatic acceptor surface crosses the donor surface exactly at the minimum of the latter. In general, this condition will not be met and, consequently, an "activation barrier" develops in the system. The introduction of such a barrier results in decreased efficiency of population transfer from donor to acceptor surfaces. We created an activation barrier by "raising up" the diabatic acceptor potential surface, without shifting its equilibrium position in nuclear coordinate space. Specifically, we changed the bias between the diabatic surface minima according to $\epsilon_0 = -\kappa \Sigma_\beta 2\tilde{c}_\beta^2/\tilde{\omega}_\beta^2$. When $\kappa=1$, the barrierless crossing case is recovered. As κ is reduced, the acceptor potential surface is lifted vertically, and consequently the energetic crossing point between the two diabatic surfaces is given by $\Sigma_\beta(1-\kappa)^2\tilde{c}_\beta^2/2\tilde{\omega}_\beta^2$ above the minimum of the + surface. This energy gives a rough estimate of the height of the activation barrier and hence lowering κ is expected to result in slower decay of $P_b(t)$. By the time that $\kappa=0.5/1.99$, deviations from the results displayed in Fig. 1 ($\kappa=1$) are clearly noticeable. The corresponding results for $\kappa=0.5/1.99$ are shown in Fig. 4. In each panel, the results of the GR approximation [in Fig. 4(a)] or NGR approximation [in Figs. 4(b)–4(e)] are compared to exact path integral results. It can be seen that the accuracy of the (N)GR approximation is not quite as good as in the barrierless crossing case considered above, although its performance is still encouraging. Interestingly, it is the standard GR situation (i.e., where $y^{(0)} = -y_0$), considered in Fig. 4(a), where the approximation is least accurate. When the initial wave packet is displaced from the center of the donor potential surface, the NGR approximation does quite well at following the plateaus and drops associated with the oscillation of the bright surface wave packet. Overall, the NGR approximation for this case of crossing through the activation barrier is accurate to within about 10%–15% down to bright surface electronic probabilities of 0.3–0.35. In Fig. 5, we plot $\ln P_b(t)$ vs t for the case considered in Fig. 4. Again it is seen that after a sufficiently long time, $\ln P_b(t)$ varies linearly with time for all initial conditions studied, and the asymptotic slope is given essentially by the standard GR rate constant [cf. Eq. (2.11)].

Because the NGR approximation is intimately tied to time-dependent perturbation theory (cf. Sec. II), it is of interest to explore the extent to which it is limited to small nonadiabatic coupling strengths Δ_0. In Fig. 6, we show results for the scenario considered in Fig. 1 (the barrierless crossing case), except that the nonadiabatic coupling strength has been increased to $\Delta_0=1.0$. The decay of $P_b(t)$ is noticeably more rapid due to the stronger value of the nonadiabatic coupling strength. Perhaps surprisingly, the NGR results are quite accurate down to populations of a few percent. Even though we are far from the limit where nonadiabatic coupling can be classified as a small perturbation, the exponentiation of the short-time dynamics analyzed in detail in Sec. II proves fruitful. It is worth noting that convergence of the path integral procedure requires more spins in the equivalent Ising chain as Δ_0 is increased. The computational details of the (N)GR approximation, on the other hand, are essentially independent of the magnitude of the nonadiabatic coupling strength. Hence (N)GR type approximations may find unexpected utility in this regime.

V. DISCUSSION AND CONCLUSION

In this work, we have derived and applied a formula for computing approximate leakage of population from an initially prepared electronic state to a second, nonadiabatically coupled, electronic state. The formula is a generalization of the standard golden rule, which applies when the initial nuclear coordinate is a rovibrational eigenstate of the potential energy surface associated with the initially populated electronic state. Here, more general initial nuclear states have been considered. In particular, our result, contained in Eqs. (2.8) and (2.9), and termed the nonequilibrium golden rule formula, incorporates effects due to preparation of the initial state out of equilibrium with respect to the nuclear coordinates. For simplicity, we have assumed that the process is dominated by "one-way leakage," i.e., no backflow of probability to the initially prepared electronic state. This assumption, which is expected to be applicable in many important cases, e.g., the exothermic regime of electron transfer reactions, makes the exponential expression in Eq. (2.9b) valid for relatively long times (on the time scale of the electronic transition).

To establish the accuracy of the nonequilibrium golden rule formula, application was made to a spin–boson model of inner sphere electron transfer. The model introduced by Garg *et al.* for transition out of the equilibrium nuclear state of the Donor electronic state[20] was extended to include initial conditions corresponding to nonequilibrium preparation on the donor surface. The predictions of the nonequilibrium golden rule were found to agree well with exact path integral results for a wide range of initial distortions of the initial nuclear wave packet from its equilibrium configuration.

A number of extensions of the themes developed in this work would be of useful. First, the inclusion of electronic population "backflow" to the initially populated state is necessary to treat important cases such as the "symmetric case" of equivalent donor and acceptor moieties. Presumably, a

Downloaded 17 Mar 2004 to 132.66.16.34. Redistribution subject to AIP license or copyright, see http://jcp.aip.org/jcp/copyright.jsp

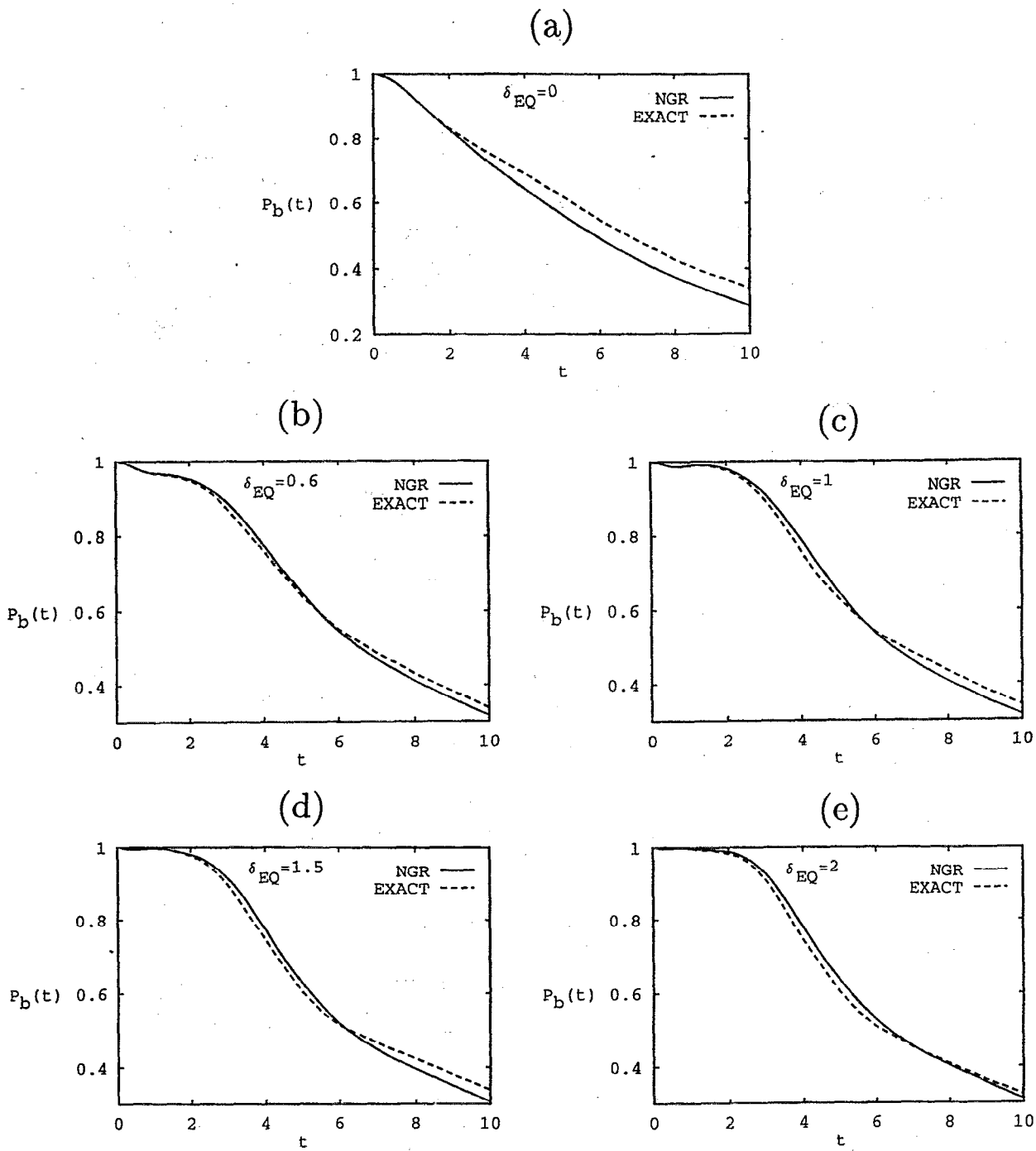

FIG. 4. $P_b(t)$ obtained from the nonequilibrium golden rule formula, indicated by a solid line, is compared with exact results (indicated by a dashed line) for the ET Hamiltonian discussed in text with vertical displacement of the (acceptor) surface $\epsilon_0=-0.5$. (This corresponds to a significant barrier for the ET process.) The nonadiabatic coupling strength is $\Delta_0=0.6$. In (a), the initial wave packet is at equilibrium on the bright surface. (b)–(e) show results for the same series of initial wave packet displacements considered in Fig. 1.

time-dependent version of the "backward" rate constant that arises in standard golden rule or master equation treatments[9] can be constructed. Another interesting generalization would be to the case of more than two nonadiabatically coupled electronic states. There is, e.g., extensive speculation that the electron transfer in the photosynthetic reaction center proceeds via an intermediate state associated with a bridging chlorophyll species.[26] If vibronic interactions are important in this electron transfer process, it may be necessary to treat effects due to nonequilibrium preparation of the nuclear coordinates on the donor potential surface. Yet another question concerns the relationship between the optical preparation process and the electronuclear dynamics which follows this preparation step. If the optical pulse duration is comparable

Downloaded 17 Mar 2004 to 132.66.16.34. Redistribution subject to AIP license or copyright, see http://jcp.aip.org/jcp/copyright.jsp

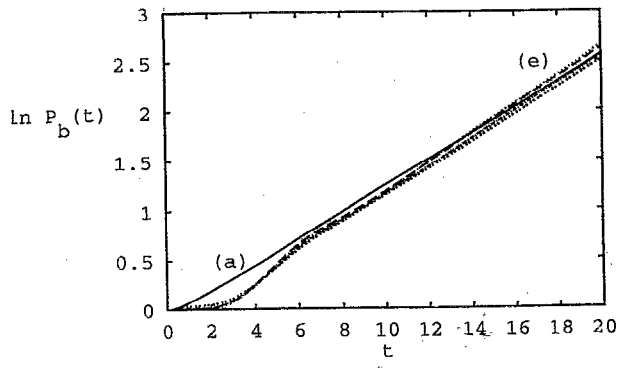

FIG. 5. $P_b(t)$ versus time for the ET system considered in Fig. 4. Data are taken from NGR computations. All curves have essentially the same asymptotic slope, consistent with the standard golden rule rate. Curves corresponding to the displacements shown in Figs. 4(a) and 4(e) are indicated on the graph as (a) and (e), respectively.

to, say, the time scale of vibrational relaxation on the bright or donor state, then it should be considered on the same dynamical footing as the electronuclear motion. In this case, the pulse preparation step needs to be folded into the evolution of the electronuclear motion according to the time-dependent Schrödinger equation. For all these more elaborate processes, as well as the simpler one considered directly in the paper, the essential simplicity of the nonequilibrium golden rule prescription opens the way to a variety of interesting condensed phase applications.

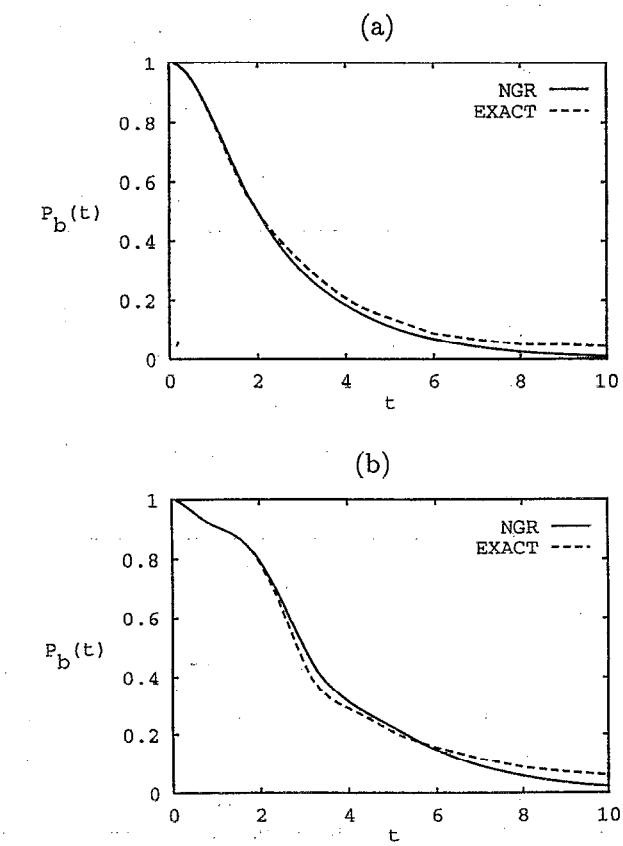

FIG. 6. $P_b(t)$ for the case of the "barrierless crossing" ET system considered in Fig. 1, except that here the nonadiabatic coupling Δ_0 is increased to the value 1.0. In (a) the wave packet is initially in equilibrium position on the + (donor) surface. In (b) the initial wave packet displacement is $\delta_{eq}=1.0$.

Note added in proof. After this paper was accepted for publication we learned of work by L. D. Zusman and A. B. Gelman on the optical absorption spectrum of a solvating electron [Opt. Spectrosc. (USSR) **53**, 248 (1982)] in which formulas similar to our Eq. (2.8) were obtained. The focus of the two articles is, however, much different. In this paper we have pointed out the potential for semiclassical calculation of time-dependent rate constants for interacting many-body systems, and the ability to extend the short-time perturbation theory analyses by appropriate processing of the short-time data. In addition, an extensive application to the GOA model of inner sphere electron transfer, including numerically exact Path Integral solutions that demonstrate the utility of the nonequilibrium golden rule procedure, is novel. We thank Dr. L. Zusman for bringing his work to our attention.

ACKNOWLEDGMENTS

AN thanks Professor H. Metiu and Professor M. A. Ratner for helpful discussions, and the U.S. Israel Binational Science Foundation and the Israel NSF for financial support. R.D.C. acknowledges financial support from the National Science Foundation, Grant No. CHE-9101432, the donors of the Petroleum Research Fund, and the Camille and Henry Dreyfus Foundation. D.G.E. thanks the University of Pittsburgh for the award of an Andrew D. Mellon Predoctoral Fellowship for 1992 and 1993. Finally, the authors would like to acknowledge the warm hospitality of the Institute for Advanced Studies at the Hebrew University, Jerusalem. Some of the computations reported here were performed at the Pittsburgh Supercomputer Center.

APPENDIX: SPIN-ENUMERATION PROCEDURE FOR EVALUATION OF ELECTRONIC POPULATION DYNAMICS IN THE SPIN–BOSON MODEL

An exact calculation of the + surface population dynamics $P_b(t)$ is required in order to gauge the accuracy of the approximate calculations proposed in Sec. III. The exact calculation is based on the spin–boson path integral formalism. This formalism converts the problem of quantum mechanical evolution on nonadiabatically coupled electronic potential surfaces into a sum over configurations of a 1D Ising spin chain. As in the standard Ising model, each spin interacts with a local external field and, in addition, all pairs of spins interact. Unlike the standard Ising model, however, the spin–spin interactions are long range and both spin–spin coupling coefficients and external field parameters are complex valued. This renders evaluation of the required spin sums nontrivial. Most attempts to evaluate these sums have been based on Monte Carlo sampling.[25] Here we opt instead for direct enumeration of spin configurations. We have found this procedure to be useful in applications of the spectroscopic spin–boson model, a variant of the canonical spin–

Downloaded 17 Mar 2004 to 132.66.16.34. Redistribution subject to AIP license or copyright, see http://jcp.aip.org/jcp/copyright.jsp

boson model which is useful for computing Franck–Condon absorption spectra in systems characterized by nonadiabatically coupled excited electronic states.[27] The details are slightly different in the case of present interest, i.e., computation of electronic state population dynamics, and hence are sketched in the following paragraphs.

We wish to calculate the + surface population

$$P_b(t)=\langle +|\langle \phi_0|e^{i\hat{H}_{\rm ET}t}|+\rangle\langle +|e^{-i\hat{H}_{\rm ET}t}|\phi_0\rangle|+\rangle \tag{A1}$$

in the case of the electron transfer models such as that proposed in Sec. III [cf. also Eq. (2.2)]. Here ϕ_0 is the initial nuclear wave packet on the + electronic surface.

Insertion of a set of complete electronic states into Eq. (A1) gives

$$\begin{aligned}P_b(t)=&\sum_{s_1=\pm}\cdots\sum_{s_{N-1}=\pm}\sum_{s_{N+1}=\pm}\cdots\sum_{s_{2N-1}=\pm}\langle\phi_0|\langle +|\\&\times e^{i\hat{H}_{\rm ET}\epsilon}|s_{2N-1}\rangle\langle s_{2N-1}|\cdots|s_{N+1}\rangle\langle s_{N+1}|e^{i\hat{H}_{\rm ET}\epsilon}|+\rangle\\&\times\langle +|e^{-i\hat{H}_{\rm ET}\epsilon}|s_{N-1}\rangle\langle s_{N-1}|\cdots|s_1\rangle\\&\times\langle s_1|e^{-i\hat{H}_{\rm ET}\epsilon}|+\rangle|\phi_0\rangle,\end{aligned} \tag{A2}$$

where $\epsilon=t/N$ and $|s_i\rangle$ is an eigenstate of σ_z, i.e., $\sigma_z|\pm\rangle=\pm|\pm\rangle$. Equation (A2) is exact for any N, but a solution is only possible in the limit where $N\to\infty$. As $\epsilon\to 0$, each of the propagators may be disentangled [with errors at $\mathcal{O}(\epsilon^2)$] to give

$$\langle s_2|e^{-i\hat{H}_{\rm ET}\epsilon}|s_1\rangle\cong\mathscr{F}_{s_2,s_1}\exp(-i\epsilon\hat{h}_{+,-}), \tag{A4a}$$

where

$$\mathscr{F}_{s_2,s_1}=\begin{cases}\cos(\epsilon\Delta_0/2), & s_1=s_2\\ -i\sin(\epsilon\Delta_0/2), & s_1\neq s_2\end{cases}, \tag{A4b}$$

and

$$h_{+,-}=\begin{cases}\hat{h}_+, & s_1=+\\ \hat{h}_-, & s_1=-\end{cases}. \tag{A4c}$$

Equation (A4) actually holds for Hamiltonians of the form (3.1) with arbitrary $\hat{h}_\pm$, but in the case of direct interest has the simple form

$$h_\pm=\sum_k\left[\frac{1}{2}(p_k^2+\omega_k^2x_k^2)\pm\delta_kx_k\right]\pm\frac{\epsilon_0}{2}.$$

{Compare Eq. (4.1). For notational simplicity, we suppress the tildes here and label the oscillator modes by the index k. Furthermore, the linear shift coefficients are denoted simply by δ_k and overall additive constants are ignored [since they do not affect $P_b(t)$].} This enables us to write

$$\begin{aligned}P_b(t)=&\sum_{s_1=\pm}\cdots\sum_{s_{N-1}=\pm}\sum_{s_{N+1}=\pm}\cdots\sum_{s_{2N-1}=\pm}\mathscr{W}_C\\&\times\exp\left[i\epsilon\left(\sum_{j=0}^{N-1}s_j-\sum_{k=N}^{2N-1}s_k\right)\frac{\epsilon_0}{2}\right]\\&\times\langle\phi_0|(\hat{U}_C^b)^\dagger\hat{U}_C^f|\phi_0\rangle.\end{aligned} \tag{A5}$$

The factor $\mathscr{W}_C=\prod_{j=1}^{2N}\mathscr{F}_{s_js_{j-1}}$, and $\hat{U}_C^f$ is the time development operator for a set of linearly driven harmonic oscillator evolving according to

$$\hat{h}_k^0(x_k)+f_k(u)x_k;$$

here $\hat{h}_k^0(x_k)$ is the standard harmonic oscillator Hamiltonian for mode k, and u is the time variable. Furthermore, $f_k(u)$ is a pulse function that on the interval $j\epsilon<u<(j+1)\epsilon$ takes values of $\pm\delta_k$ if $s_j=\pm$ for $0\leqslant j\leqslant N-1$. The propagator $\hat{U}_C^b$ is defined analogously, with a pulse function that depends in an obvious way on the spin variables s_N-s_{2N-1}.

In order to calculate $P_b(t)$, we need to calculate the factor $\langle\phi_0|(\hat{U}_C^b)^\dagger\hat{U}_C^f|\phi_0\rangle$. This quantity can be obtained analytically, since the initial wave packet for each mode is a Gaussian coherent state which is to be evolved according to a linearly driven harmonic oscillator potential,[28] with a driving force defined by the spin configuration as just discussed.

Essentially the same technique described in this appendix has been used in previous calculations of spectroscopic line shapes within the spectroscopic spin–boson model.[27] The presence of both a forward and a reverse time development operator ($\hat{U}_C^f$ and $\hat{U}_C^b$) in the electronic population calculations renders calculation of $P_b(t)$ to longer times more difficult than analogous optical spectra. Effectively, it requires twice as many spins to compute the population decay as it does to calculate the value of an electronic absorption kernel at the same time value.

[1] See, e.g., K. Holtzclaw and D. W. Pratt, Chem. Phys. Lett. **118**, 375 (1985).

[2] See, for example, (a) H. Köppel, W. Domcke, and L. S. Cederbaum, Adv. Chem. Phys. **57**, 59 (1984); (b) G. Stock, R. Schneider, and W. Domcke, J. Chem. Phys. **90**, 7184 (1989); (c) U. Manthe and H. Köppel, *ibid.* **93**, 345 (1990); **93**, 1658 (1990).

[3] (a) M. O. Trulson and R. A. Mathies, J. Chem. Phys. **94**, 5741 (1990); (b) R. J. Hemley, J. I. Dawson, and V. J. Vaida, *ibid.* **78**, 2915 (1983).

[4] (a) S. Mukamel and J. Jortner, in *MTP International Review of Science*, edited by A. D. Buckingham and C. A. Coulson (Butterworth, London, 1976), Vol. 13, p. 327; (b) F. K. Fong, *Radiationless Transitions* (Springer, Berlin, 1976); (c) M. Bixon and J. Jortner, J. Chem. Phys. **48**, 715 (1968); **50**, 4061 (1970); A. Nitzan and J. Jortner, *ibid.* **57**, 2870 (1972); Mol. Phys. **24**, 109 (1972).

[5] (a) J. M. Jean, R. A. Friesner, and G. R. Fleming, J. Chem. Phys. **96**, 5827 (1992), and other references therein; (b) J. Ulstrup, *Lecture Notes in Chemistry* (Springer, Berlin, 1979), Vol. 10; (c) see, e.g., J. C. Tully, J. Chem. Phys. **93**, 1061 (1990) and references therein.

[6] J. F. Black, J. R. Waldeck, and R. N. Zare, J. Chem. Phys. **92**, 3519 (1990).

[7] (a) K. Q. Lao, M. D. Person, P. Xayariboun, and L. J. Butler, J. Chem. Phys. **92**, 823 (1990); (b) T. S. Rose, M. J. Rosker, and A. H. Zewail, *ibid.* **88**, 6672 (1988).

[8] G. Baym, *Lectures on Quantum Mechanics* (Benjamin, Reading, MA, 1973), Chap. 12.

[9] K. Blum, *Density Matrix Theory and Applications* (Plenum, New York, 1981); E. J. Heller and R. C. Brown, J. Chem. Phys. **79**, 3336 (1983); M. Sparglione and S. Mukamel, *ibid.* **88**, 3263 (1988).

[10] M. Lax, J. Chem. Phys. **20**, 1753 (1952).

[11] E. Neria and A. Nitzan, J. Chem. Phys. **99**, 1109 (1993); Chem. Phys. (in press).

[12] L. E. Fried and S. Mukamel, Adv. Chem. Phys. (in press).

[13] See, e.g., C. W. Gardiner, *Quantum Noise* (Springer, Berlin, 1991), Chaps. 5 and 6.

[14] D. W. Oxtoby, Adv. Chem. Phys. **47**, 487 (1981).

[15] (a) G. Angel, R. Gagel, and A. Laubereau, Chem. Phys. Lett. **156**, 169 (1989); Chem. Phys. **131**, 129 (1989); (b) F. Laermer, T. Elsaesser, and W. Kaizer, Chem. Phys. Lett. **156**, 381 (1989).

[16] R. Z. Zwanzig, Physica **30**, 1109 (1964) and references therein; A. G.

Downloaded 17 Mar 2004 to 132.66.16.34. Redistribution subject to AIP license or copyright, see http://jcp.aip.org/jcp/copyright.jsp

Redfield, Adv. Magn. Reson. **1**, 1 (1965); see also Ref. 5(b) and references therein.
[17] A. Nitzan and J. Jortner, Chem. Phys. Lett. **15**, 350 (1972); J. Chem. Phys., **58**, 2412 (1973).
[18] M. L. Goldberger and K. Watson, *Collision Theory* (Krieger, New York, 1975).
[19] (a) A. J. Leggett, S. Chakravarty, A. T. Dorsey, M. P. A. Fisher, A. Garg, and W. Zwerger, Rev. Mod. Phys. **59**, 1 (1987); (b) A. O. Caldeira and A. J. Leggett, Ann. Phys. (NY) **149**, 374 (1983).
[20] A. Garg, J. N. Onuchic, and V. Ambegaokar, J. Chem. Phys. **83**, 4491 (1985); see also, J. N. Onuchic, *ibid.* **86**, 3925 (1987); J. N. Onuchic, D. N. Beratan, and J. J. Hopfield, J. Phys. Chem. **90**, 3707 (1986).
[21] For the remainder of the paper, the term "nonadiabatic" will be used to describe all nonradiative coupling effects including, e.g., spin–orbit interactions.
[22] We have opted to use radiationless transition language in our presentation of the nonequilibrium golden rule. The same results apply directly to electron transfer in the nonadiabatic regime. Indeed, the illustrative example presented in Sec. IV is drawn from the electron transfer literature.
[23] E. J. Heller, Acc. Chem. Res. **14**, 368 (1981).
[24] R. E. Zwanzig, J. Stat. Phys. **9**, 215 (1973).
[25] (a) E. C. Behrman, G. A. Jongeward, and P. G. Wolynes, J. Chem. Phys. **79**, 6277 (1983); (b) C. H. Mak and D. Chandler, Phys. Rev. A **44**, 2352 (1991); (c) C. H. Mak, Phys. Rev. Lett. **68**, 899 (1992).
[26] See, e.g., *The Photosynthetic Bacterial Reaction Center*, edited by J. Breton and A. Vermeglio (Plenum, New York, 1988); J. N. Gehlen, M. Marchi, and D. Chandler, Science **263**, 499 (1994).
[27] (a) R. D. Coalson, J. Chem. Phys. **86**, 995 (1987); (b) Phys. Rev. B **39**, 12502 (1989); (c) J. Chem. Phys. **94**, 1108 (1991).
[28] See, e.g., P. Pechukas and J. C. Light, J. Chem. Phys. **44**, 3897 (1965); these techniques are utilized extensively in Ref. 27.

Downloaded 17 Mar 2004 to 132.66.16.34. Redistribution subject to AIP license or copyright, see http://jcp.aip.org/jcp/copyright.jsp